

# 1 Substrate evaporation drives 2 collective construction in termites

3 G. Facchini<sup>1,2\*</sup>, A. Rathery<sup>2</sup>, S. Douady<sup>3</sup>, D. Sillam-Dussès<sup>4</sup>, A. Perna<sup>2</sup>

\*For correspondence:  
[giulio.facchini@ulb.be](mailto:giulio.facchini@ulb.be) (GF)

4 <sup>1</sup>Life Sciences Department, University of Roehampton, London SW15 4JD, United  
5 Kingdom; <sup>2</sup>Service de Chimie et Physique Non Linéaire, Université Libre de Bruxelles,  
6 Brussels 1000, Belgium; <sup>3</sup>Laboratoire Matière et Systèmes Complexe, Université Paris  
7 Cité, Paris 75205 Paris Cedex 13, France; <sup>4</sup>Laboratoire d'Ethologie Expérimentale et  
8 Comparée, LEEC, UR 4443, Université Sorbonne Paris Nord, Villetaneuse 93430, France

---

10 **Abstract** Termites build complex nests which are an impressive example of self-organization.  
11 We know that the coordinated actions involved in the construction of these nests by multiple  
12 individuals are primarily mediated by signals and cues embedded in the structure of the nest  
13 itself. However, to date there is still no scientific consensus about the nature of the stimuli that  
14 guide termite construction, and how they are sensed by termites. In order to address these  
15 questions, we studied the early building behavior of *Coptotermes formosanus* termites in artificial  
16 arenas, decorated with topographic cues to stimulate construction. Pellet collections were evenly  
17 distributed across the experimental setup, compatible with a collection mechanism that is not  
18 affected by local topography, but only by the distribution of termite occupancy (termites pick  
19 pellets at the positions where they are). Conversely, pellet depositions were concentrated at  
20 locations of high surface curvature and at the boundaries between different types of substrate.  
21 The single feature shared by all pellet deposition regions was that they correspond to local  
22 maxima in the evaporation flux. We can show analytically and we confirm experimentally that  
23 evaporation flux is directly proportional to the local curvature of nest surfaces. Taken together,  
24 our results indicate that surface curvature is sufficient to organize termite building activity, and  
25 that termites likely sense curvature indirectly through substrate evaporation. Our findings  
26 reconcile the apparently discordant results of previous studies.

---

## 28 Introduction

29 Termites are known for their ability to build some of the most complex nests and shelters found in  
30 nature (*Hansell, 2005; Perna and Theraulaz, 2017*). The construction of these structures is achieved  
31 through the collective actions of multiple individual workers (up to thousands or millions in large  
32 termite colonies) each performing the collection, transportation and deposition of elementary pel-  
33 lets. In order to produce functionally meaningful structures, it is essential that all these different  
34 workers operate in a coordinated, coherent way, each continuing the work started by their colony  
35 mates, rather than undoing it.

36 Termites rely on individual memory and proprioception to guide their behavior (see e.g. *Bardunias*  
37 *and Su, 2009a*), but these individual abilities are considered not sufficient to explain nest construc-  
38 tion more generally. Instead, it is believed that building activity is largely guided by signals and  
39 cues embedded directly in the structure of the nest itself, through a regulation principle identified  
40 for the first time by Grassé, who named it *stigmergy* (*Grassé, 1959; Camazine et al., 2001*).

41 In stigmergy-mediated nest-building, the probability for an individual insect to pick or to drop a  
42 pellet at a particular location is modulated by stimuli encountered at that location, such as the ge-

ometry of a growing pillar, or the presence of a chemical signal released by the queen or by other workers.

However, several years since Grassé's early observations, there still isn't a consensus on the exact nature of the stigmergic stimuli involved in regulating termite construction. Pheromones might be implicated in this regulation. *Bruinsma (1979)* found evidence for the role of a building pheromone released by the queen in the construction of the royal chamber of the termite *Macrotermes subhyalinus*. Computer simulation studies, aimed at reproducing the building behavior of termites and ants, also assume the existence of a "cement pheromone" added to the building material (*Khuong et al., 2011, 2016; Heyde et al., 2021*). In these simulation studies the main and essential role of a cement pheromone is to allow initial pellet depositions to continue growing by differentiating them from regions of pellet collection, through differential pheromone marking. Experimental evidence in support for such cement pheromone in termite construction is weak: while individual workers can recognize freshly deposited nest material, they could simply be attracted to an unspecific colony odor while exhibiting the same behavioral patterns that they would exhibit also in the absence of chemical marking (*Petersen et al., 2015*). In other words, it is not clear if cement pheromones are required to drive termite building activities, or unspecific chemical cues would be sufficient, and it is also unclear if chemical stimuli modulate the building behavior of termites directly, or only indirectly, by affecting their density of presence.

Recent experimental studies by various authors have indicated that morphological and environmental features associated with some nest structures are strong stimuli that could by themselves guide termite construction activity. These include elevation (*Fouquet et al., 2014*), humidity gradients (*Soar et al., 2019*), and surface curvature (*Calovi et al., 2019*). The strong attractiveness of digging sites for termite aggregation means that in all these studies digging and deposition actions mostly come in pairs, which prevents us from identifying the genuine cues for pellet collection and deposition (*Bardunias and Su, 2009b, 2010; Fouquet et al., 2014; Green et al., 2017*). For example, in *Calovi et al. (2019)* termites are shown to preferentially aggregate in concave regions of a surface and they would simply rearrange nest material (both digging and building) at those locations. Even if digging sites provide a template for pellet deposition (*Fouquet et al., 2014; Green et al., 2017*), and for this reason digging and construction often co-localize in space, it is clear that building and digging cannot completely overlap, or the two activities would simply cancel one the effect of the other: termites must be able to differentiate between the sites of these contrasting activities through digging- or building-specific cues.

Some of the published computer simulation models of termite nest-building do not require a specific construction pheromone and assume instead that termites respond to cues naturally embedded in the nest structure itself. For example, the model proposed in *Ocko et al. (2019)* indicates that a generic "colony odour" undergoing advection and diffusion within the nest could provide a sufficient cue for determining the overall mound shape, so leaving a possible role of a construction pheromone only for the structuring of small scale nest features such as pillars and walls. *Facchini et al. (2020)* further proposed a model in which also small scale nest features can be produced in the absence of a construction pheromone, by assuming that termites respond to the local curvature of these emerging nest features. While these models reproduce a number of structures observed in real termite nests, the building rules implemented in the models are not empirically validated from direct observations of the building behavior of termite workers. As it stands, there is no conclusive evidence that the rules implemented in these models reflect the actual nest-building strategies of termites.

Here we aim to test whether geometric and physical cues embedded in the nest material are sufficient to explain termite construction. Specifically we want to disentangle how elevation, surface curvature, and substrate evaporation affect pellet deposition and collection. We do this by combining three different approaches. (i) We perform building experiments in which populations of termites are confronted with pre-existing building cues such as pillars, walls, and pre-made pellets of building material unmarked with pheromones. Using video-tracking, we monitor the presence

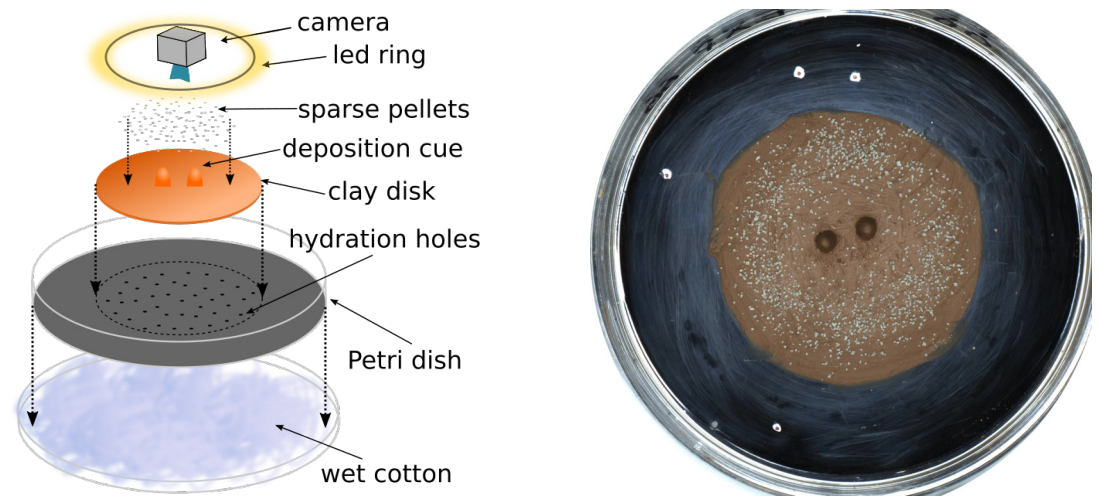


**Figure 1.** Sketch of the experimental setup (left) and snapshot of one experiment (E66) before termites were added to the setup (right). The white marks on the picture give the scale of the setup, with the distance between successive marks being 1, 3, and 5 cm.

94 of individual termites and we implement high throughput video-analysis to detect the time and  
95 location of individual pellet collection and deposition events. These experiments allow us to test  
96 the specific role played by each cue on stimulating pellet collection, pellet deposition, or termite  
97 aggregation. (ii) By running a computational model of nest building (*Facchini et al., 2020*) directly  
98 on the same structures that we provide to termites (obtained from 3D scans of our experimental  
99 setups) we can test exactly what building patterns we should expect under the simple assumption  
100 that termite depositions are driven by the local curvature of nest surfaces as the only construction  
101 cue. (iii) Finally, we develop a “chemical garden” experiment, on identical setups to those offered to  
102 termites, that allow us to visualize the sites of stronger water evaporation on the surface of the built  
103 structure. Overall, our approach allows us to demonstrate, both analytically and experimentally,  
104 the relation between deposition probability, surface curvature, and evaporation.

## 105 Results

106 Below, we report the observations of *de novo* building experiments performed with small experi-  
107 mental groups of *Coptotermes formosanus* termites confronted with a thin disk of humid clay cov-  
108 ered with pre-made pellets unmarked with pheromones and decorated with pre-prepared clay  
109 features. In the first series of experiments the pre-prepared features were two pillars at the center  
110 of the clay disk as shown in figure 1.

111 Pellet collection activity was distributed homogeneously all over the clay disk that we provided  
112 at the center of the experimental arena. Conversely, deposition activity was concentrated at the  
113 tips of pre-existing pillars, and along the edges of the clay disk itself. Figure 2A reports the heatmap  
114 of cumulative depositions  $P(D)$  and collections  $P(C)$  for one experiment (E66) with two pillars as  
115 topographic cues. A snapshot of the same experiment is reported in figure 3A. In figure 2B, we also  
116 report the same results for five experiments for which our analyses were most reliable because of  
117 the absence of spontaneous digging. Across all experiments, collections were widely distributed  
118 across the clay disk (i.e. where initial pellets are) while depositions were peaked at radii  $R \sim 0.4$  cm  
119 and  $R \sim 2.5$  cm which correspond to the top of pillars and to the edges of the experimental arena.  
120 Thus, termites do not show a preference for where they collect pellets while they target specific  
121 regions when depositing, which suggests that those regions must express a strong stimulus for  
122 deposition.

123 To validate this hypothesis, we analyzed how building activity is related to the termite occu-  
124 pancy in the experimental setup. In figure 2D, we report the normalized cumulative occupancy of

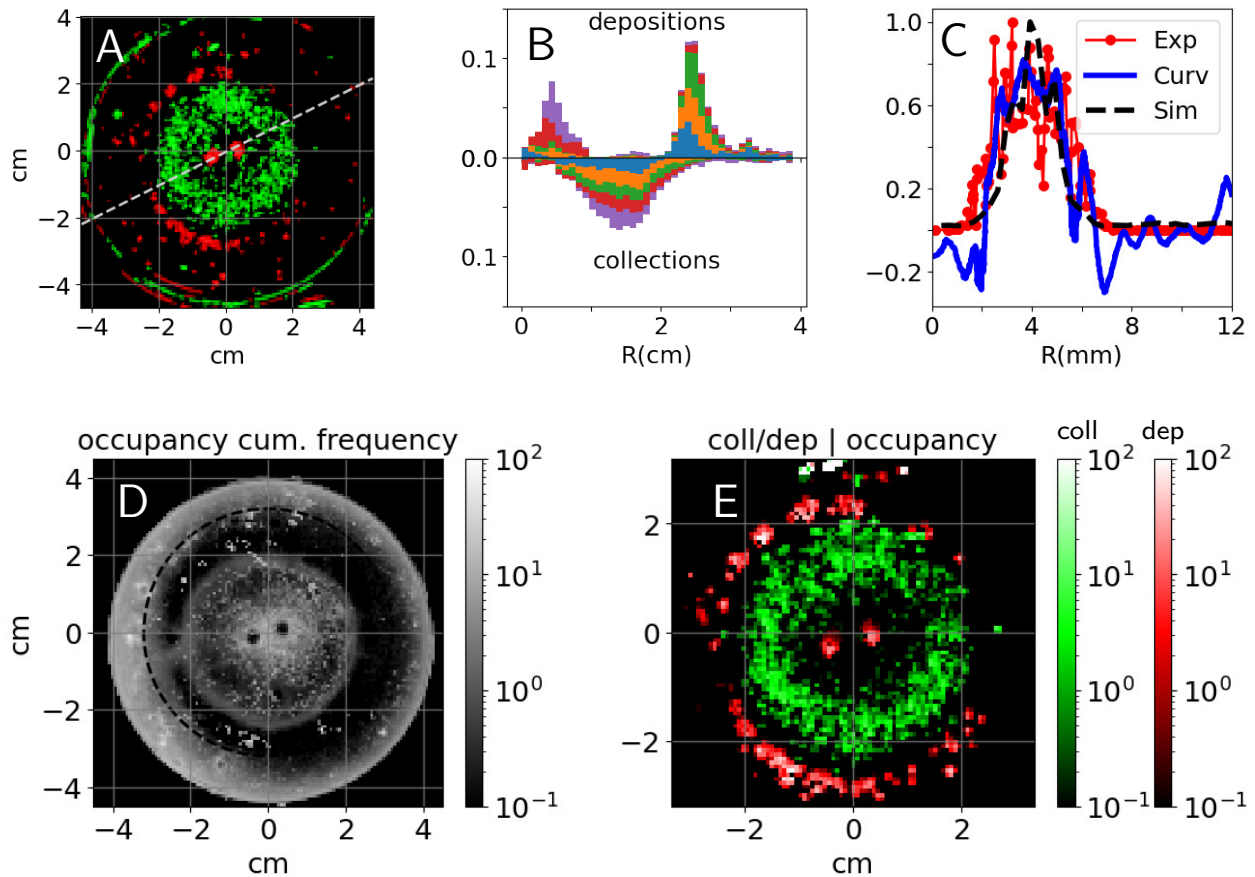


**Figure 2.** Top: (A) cumulative heatmaps of deposition ( $P(D)$ ; red) and collection activity ( $P(C)$ ; green) normalized by their respective mean values for one experiment (E66), colorbars are the same as in panel (E); (B) cumulative depositions (top) and collections (bottom) per unit area as a function of the Petri dish radius for experiments E58, E63, E65, E66, and E76, all histograms have been normalized and sum up to 1; (C) comparison among experimental depositions (in red), surface curvature (in blue) shown in Fig. 3C, and depositions predicted by simulations (black) shown in Fig. 3C, all the quantities are computed along the radial cut shown in panel (A), depositions are normalized by their maximum value and curvature is in  $\text{mm}^{-1}$ ; (D) cumulative occupancy heatmap normalized by its mean value for E66; (E) depositions ( $P(D|O)$ ; red) and collections ( $P(C|O)$ ; green) conditional to cumulative normalized occupancy for E66.

125 termites  $P(O)$  in the experimental setup. Occupancy is high close to the pillars and to the Petri  
 126 dish walls, has intermediate values within the clay disk, and drops at the top of the pillars and right  
 127 outside of the clay disk (i.e. precisely where deposits are recorded). To estimate how position and  
 128 building activity are related, we report the conditional probabilities of depositing  $P(D|O)$  and col-  
 129 lecting  $P(C|O)$  given termite occupancy. They are defined as the ratio between  $P(D)$  to  $P(O)$  and  
 130  $P(C)$  to  $P(O)$  as reported in figure 2E, and explained in section S.III of the Supplementary Informa-  
 131 tion (SI). The probability  $P(D|O)$  reaches values 10 times larger than  $P(C|O)$  which confirms that  
 132 our topographic cues and the clay disk edges specifically drive early building activity.

133 Focusing on topographic cues, we observe that pillar tips are the most curved part of the topog-  
 134 raphy but also the most elevated one. In order to disentangle the respective roles of curvature and  
 135 elevation in guiding pellet deposition, we considered a different setup where a thin wall replaced  
 136 the two pillars in the center of the arena as shown in figure 3B. This way, the top edge of the wall  
 137 is still a region of both high elevation and high surface curvature but elevation is constant every-  
 138 where while curvature has local maxima at the tips. We report that the top edge attracted many  
 139 deposits, but pellet deposition focused at the wall tips pointing to curvature, rather than elevation,  
 140 as the dominant cue in 7 out of 11 experiments (SI table S1).

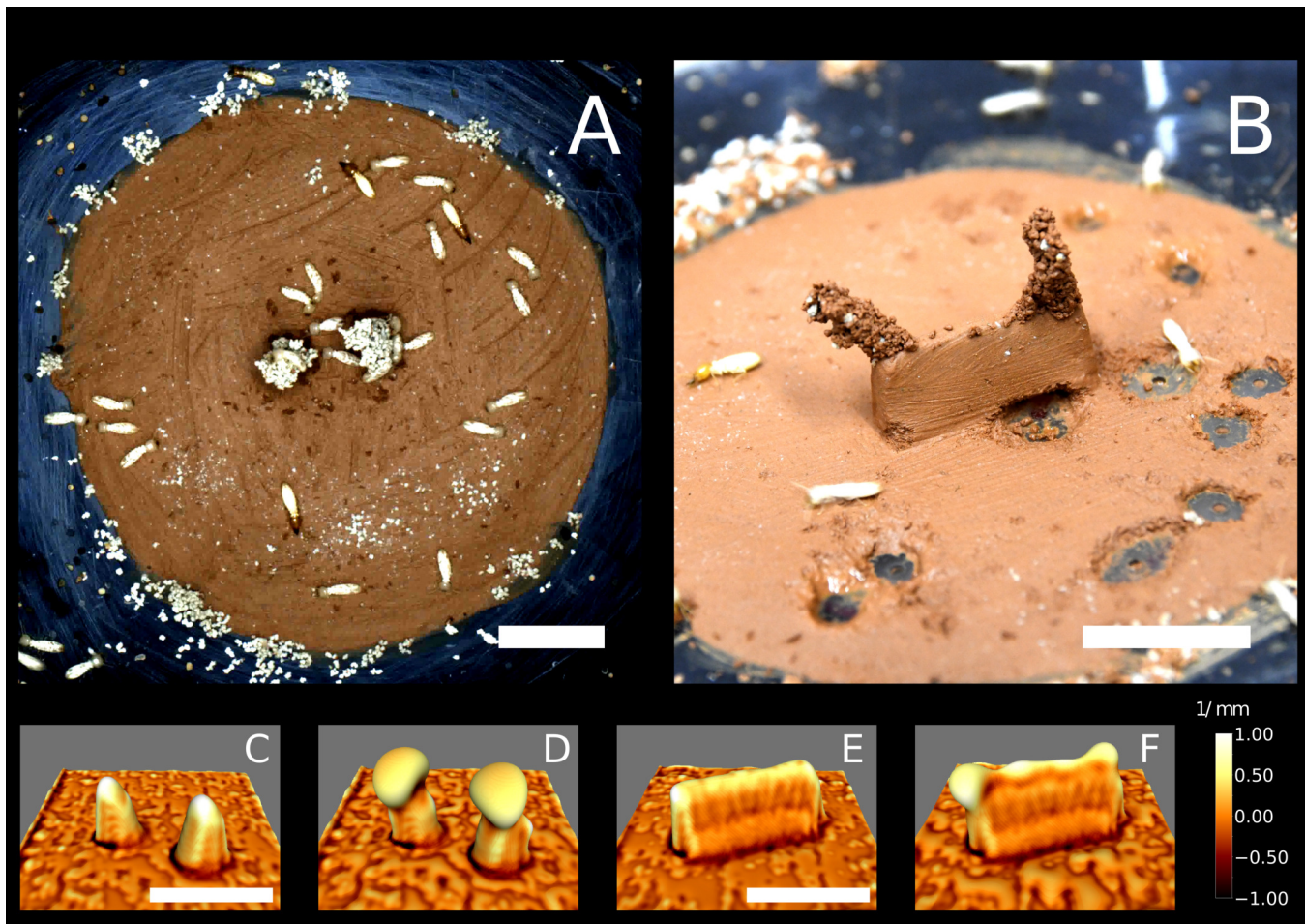


**Figure 3.** Top row: snapshots of a building experiment with “pillars” cue (E66) (A) and a building experiment with “wall” cue (E78, in B). Bottom row: snapshots of 3D simulations initiated with copies of the experimental setup E66 (C,D) and E78 (E,F) in which nest growth is entirely determined by the local surface curvature (based on our previously described model (Facchini *et al.*, 2020)). Snapshots C and E refer to  $t=0$ , D and F refer to  $t=9$  (dimensionless). The color map corresponds to the value of the mean curvature at the interface air-nest. White indicates convex regions and black indicates concave regions. The scale bars correspond to 1 cm.

141 We wanted to further test to what extent the patterns that we observe are consistent with ter-  
142 mites only responding to local substrate curvature, as opposed to responding also to other cues.  
143 To this end, we ran a model of nest construction that we have previously developed (Facchini *et al.*,  
144 2020) using 3D scans of the experimental arena – before the introduction of termites – as a start-  
145 ing template for the simulations (see Materials and Methods for simulation details). The simulation  
146 model implements one single construction rule which is a building response to local surface cur-  
147 vature and as such informs us about the possible building outcome that we could expect under  
148 the simplified assumption that construction is driven by surface curvature only, in the absence of  
149 any other cues. This yielded the results shown in figure 3C-F. Experiments and simulations show a  
150 fair agreement as pellet depositions and initial growth concentrate in the same regions which are  
151 those where the surface is the most convex, as depicted in white in figures 3C-F. For a more quan-  
152 titative comparison in Fig. 2C we report a radial cut of: the deposition heatmap (red), the surface  
153 curvature (blue) and the amount of depositions predicted by the simulations (black; see SI section  
154 S.VII for technical details of this analysis). The three curves show a good agreement and they all  
155 are peaked close to  $R = 4$  mm which corresponds to the pillar tips.

156 The similarity between experimental results and curvature-based simulations supports the idea  
157 that, at least on a first approximation, surface curvature alone is a sufficient cue that could guide

158 termite depositions.

159 The edges of the clay disk were not included in the simulations because we could not charac-  
160 terize them properly with our scanning device (see SI, section S.III). However, in additional experi-  
161 ments with no topographic cues (SI, Fig. S3) most depositions happened precisely at the edges of  
162 the clay disk. It is possible that the very small edge of the clay disk provided a sufficient stimulus,  
163 in terms of local curvature, to elicit pellet depositions. However, the curvature cue was likely very  
164 weak at those locations as edges were smoothed out to gently match the surface of the Petri dish.  
165 Thus, we expect this region to bear a cue other than curvature (or elevation) which is also attractive  
166 for pellet depositions.

167 Trying to identify this additional building cue, we recall that the clay disk is maintained con-  
168 stantly humid. The edges of the disk arena mark then the limit between a humid region and the  
169 surrounding dry periphery. Also, the clay tone remained unchanged during experiments which  
170 suggests that moisture is constantly evaporating from the clay disk while being replenished in wa-  
171 ter from below, and that the overall process is stationary. To confirm this hypothesis, we measured  
172 the value of humidity and temperature both in the central and peripheral regions. We observed  
173 a net increase in humidity and a net decrease in temperature coming from outside to inside the  
174 clay disk which is the footprint of evaporation (SI, Fig. S4). Inside and outside the clay disk, both  
175 quantities remained relatively stable indicating that the system is roughly at equilibrium. Evapo-  
176 ration is a complex process, but close enough to the evaporating substrate, humidity transport  
177 happens by diffusion (*Langmuir, 1918; Hisatake et al., 1993*) and it is hence fully determined by  
178 the humidity gradient. In agreement with previous studies (*Soar et al., 2019*), we can show with  
179 scaling arguments that our termites live in such a *viscous boundary layer* (see SI, section S.IX). We  
180 can hence focus our attention on this specific region without loss of generality. For example, the  
181 humidity transition at the edges of the clay disk implies that the humidity gradient must be pro-  
182 nounced there and evaporation with it. In the diffusive regime, the evaporation flux is directly  
183 proportional to the surface curvature of the evaporating substrate (see SI, section S.VIII for a math-  
184 ematical proof). As a demonstration for our topographic cues, we have computed the equilibrium  
185 solution for the humidity field  $h$  in a cubic volume bounded by pillars and wall experimental tem-  
186 plates at the bottom. In the diffusive regime, this corresponds to solving the Laplace equation  
187  $\Delta h = 0$  while imposing a humid condition  $h = 1$  at the bottom boundary, and a dry condition  $h = 0$   
188 at the top boundary (see S.VI in the SI for details). In figure 4A and 4B we have reported the contour  
189 plot of the magnitude of the humidity gradient  $\nabla h$  for this stationary solution. We can observe that  
190 the humidity gradient is maximum at the tip of pillars and at the lateral tips of the wall top edge,  
191 that are the most curved parts in the two different cues (see figures 3C and 3E for a direct compar-  
192 ison). As such, curvature and evaporation are two completely interchangeable stimuli everywhere  
193 except at the edge of the clay disk, where the transition between clay and perspex material cor-  
194 responds to a strong humidity gradient in spite of weak surface curvature. We then propose that  
195 evaporation flux can explain by itself the deposition patterns observed in our experiments.

196 To support this hypothesis we designed a chemical garden experiment that allows us to visu-  
197 alize the evaporation field in our setup. We prepared identical experimental setups as those used  
198 with termites, but this time we did not put any termites in the experimental arena. Instead we  
199 replaced the deionized water that was used to humidify the clay in the termite experiments with a  
200 saturated saline solution of water and  $\text{NaHCO}_3$ . In this configuration, water evaporation is accom-  
201 panied by the deposition of salt, which allows to build a chart of evaporation flux. Typical results  
202 are shown in figure 4C and 4D. Salt deposits appear in the form of white traces or bumpy defor-  
203 mations of the clay surface. Remarkably the distribution of the salt deposits matches very closely  
204 the regions of highest building activity by termites, both being more pronounced at the edge of  
205 the clay disk and at the top of topographic cues (pillar and walls). This result indicates that termite  
206 deposition probability covaries with the evaporation flux, which is consistent with our hypothesis  
207 of evaporation as the strongest cue for deposition. One may notice that salt traces are less pro-  
208 nounced on the wall (Fig. 4D) than on the pillars (Fig. 4C). This is consistent with the amplitude of

209 the humidity gradient in a stationary diffusive regime as shown in figure 4B and 4A respectively;  
210 the maximum amplitude of the gradient is weaker in the wall case. Also one observes that while  
211 having its maxima at the lateral tips, the humidity gradient is strong all over the top edge of the  
212 wall. Possibly this could explain why in the case of wall cues there is a comparatively much larger  
213 variability in the patterns of termite construction (see SI Fig. S2). When termites are confronted  
214 with the 'wall' cue they are likely to start pellet depositions at the wall tips, but initial pellet depositions  
215 started at other locations on the top edge do occur. Likely, when this happens, these initial  
216 depositions are then preserved and reinforced by positive feed-back mechanisms.

217 Note that, in the picture of depositions being attracted by evaporation flux, depositions observed  
218 at the edges of the clay disk, also agree with our previous growth model driven only by  
219 curvature (*Facchini et al., 2020*). In fact, the edge of the clay disk is almost flat (weak convexity)  
220 for a termite walking across, but it is also a thin cusp (high convexity) of humid material which is  
221 strongly evaporating, similarly to what happens at the edge of a liquid drop and causes the formation  
222 of well known coffee stains (*Deegan et al., 1997*). For a better comprehension, this apparent  
223 contrast is explained in the sketch of figure S6 (SI).

## 224 Discussion

225 Several experimental studies have tried to identify the cues that mediate termite construction,  
226 alternately indicating elevation (*Fouquet et al., 2014*), digging activity (*Green et al., 2017*), humidity  
227 transitions (*Soar et al., 2019; Bardunias et al., 2020*), or surface curvature (*Calovi et al., 2019*) as  
228 the relevant stimuli to drive pellet depositions. However, the fact that termites often concentrate  
229 their building activity in the immediate proximity of digging sites (*Fouquet et al., 2014; Green et al.,*  
230 *2017; Bardunias and Su, 2009b, 2010*) did not allow identifying which of these stimuli were specific  
231 digging and building cues, or simply generic cues for termite activity and aggregation. The cues  
232 themselves identified by different studies were different, leaving it unclear which, if any, were the  
233 relevant ones sensed by termites.

234 Here, by providing loose and unmarked pellets, we were able to prompt building activity with-  
235 out digging and to quantify collections and depositions as separate actions. We observed that  
236 all pellets are progressively displaced and that collections happened in a relatively random fash-  
237 ion. On the contrary, depositions concentrated at specific parts of the experimental arena which  
238 are the tips of the topographic cues and the edges of the clay disk. The conditional probability  
239 of deposition given termite occupancy is high there, indicating that those regions precisely drive  
240 termite depositions rather than generically attracting termite aggregation. The alternative use of  
241 pillars and walls as topographic cues allowed us to disentangle the role of elevation and curvature  
242 and pointed towards curvature as the most attractive stimulus for deposition. By simulating the  
243 building process with a model in which construction activity is driven by curvature only (*Facchini*  
244 *et al., 2020*), we obtained a good match with experimental results, indicating that curvature alone  
245 is sufficient to explain pellet depositions on topographic cues (pillars and walls).

246 Surface curvature is a powerful morphogenetic organizer for 3D structure formation as it can  
247 drive the formation of pillars, walls and convoluted surfaces (*Facchini et al., 2020*), all features that  
248 are observed in the nests of various termite species. Here, we are able to demonstrate a close  
249 coupling between surface curvature and the flux of evaporation from a surface, so providing a  
250 link to a possible stimulus sensed directly by termites. This also allows us to reconcile previous  
251 discordant results pointing alternately to curvature (*Calovi et al., 2019; Facchini et al., 2020*) or  
252 to humidity (*Soar et al., 2019; Bardunias et al., 2020*) as the relevant stimuli. The idea itself of a  
253 relation between curvature and evaporation is not new, as already a century ago, *Langmuir (1918)*  
254 showed that close enough to the surface of a water droplet, evaporation scales as the inverse of the  
255 radius (i.e. as the mean curvature) of the droplet (SI, section S.VIII.A). Our system is more complex  
256 than isolated spheres but our calculations in S.IX (SI) show that a relation between evaporation and  
257 curvature still holds at the termite scale.

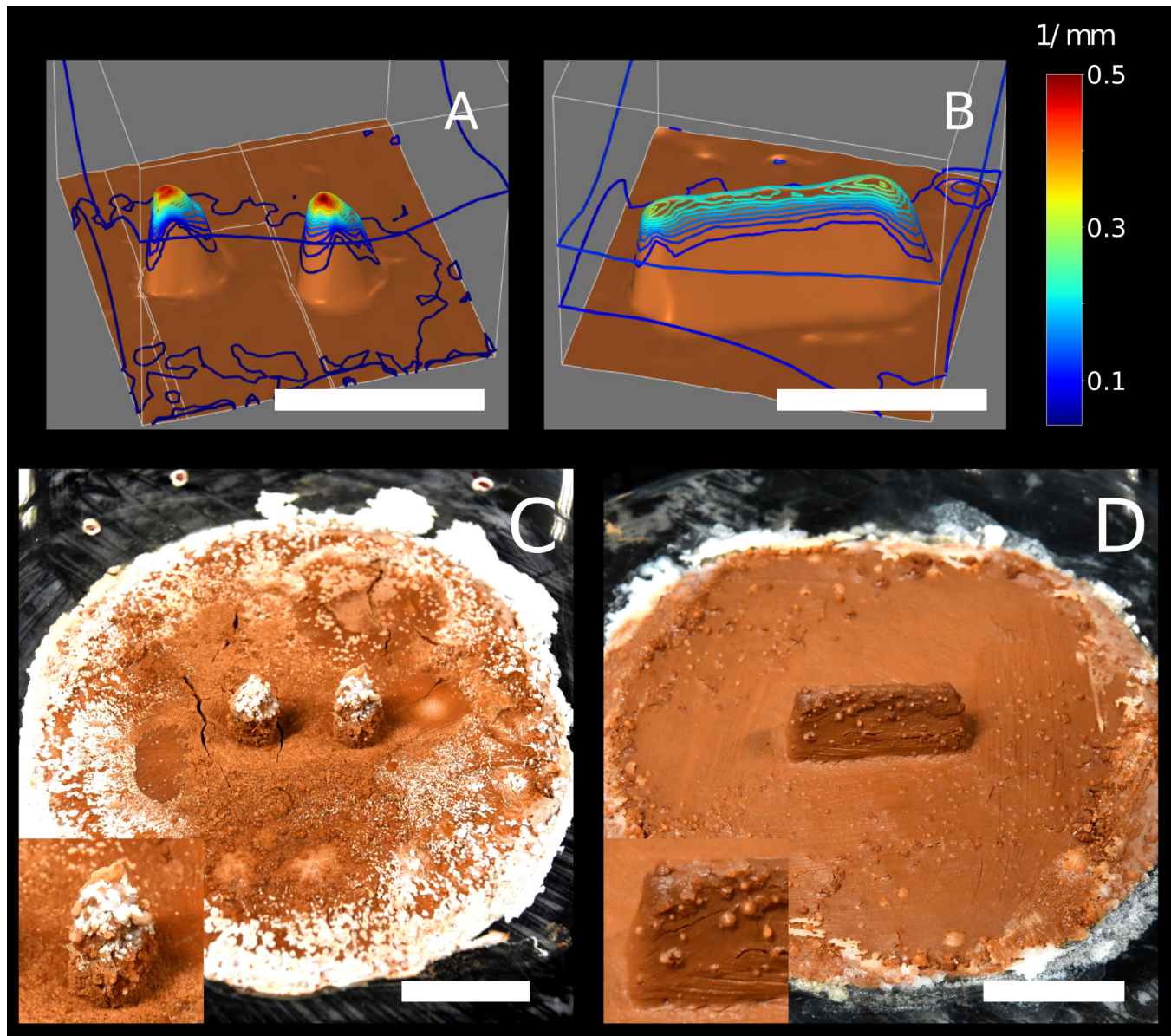


**Figure 4.** Top row: contour of the humidity gradient  $\nabla h$  obtained solving the Laplace equation  $\Delta h = 0$  in a cubic domain with a humid boundary  $h = 1$  (in brown) where the boundary is mapped from 3D scans of the experimental setup in E66 (A) and E78 (B). Humidity  $h$  is considered dimensionless here. Pillar tips are associated with a strong humidity gradient; the top of the wall, and particularly the two corners, are also associated with a humidity gradient, although the gradient is not as strong as at the pillar tips. Bottom row: snapshots of chemical garden experiments initiated with “pillars” cue (C), and with “wall” cue (D). The scale bars correspond to 1 cm.

258 As a further, direct, confirmation of our hypothesis, our chemical garden experiments clearly  
259 show that the correspondence between surface curvature and evaporation flux is relevant in our  
260 experimental setup.

261 It is well known that termites are particularly sensitive to the humidity of their environment,  
262 partly because their soft cuticle puts them in constant danger of desiccation. It is hence not sur-  
263 prising that they may sense and respond to humidity gradients with their behavior. In fact, recent  
264 field and laboratory experiments have shown that humidity can affect the overall building activity  
265 (Carey *et al.*, 2019) of termites and trigger nest expansion events (Bardunias *et al.*, 2020; Carey  
266 *et al.*, 2021). Even more interestingly, Soar *et al.* (2019) showed that moisture flux favors termites  
267 building activity (both digging and deposition). Our experiments confirm this trend and suggest



268 that moisture variations not only prompt or inhibit termite building activity, but constitute a local  
269 blueprint for construction.

270 Our experiments do not support a role for a putative cement pheromone, added by termites to  
271 the building material, which would stimulate pellet depositions. In fact, construction occurred reli-  
272 ably on our provided building cues, even if they only comprised fresh clay and sterilized pellets with  
273 no pheromone markings. Our simulations further indicate that qualitatively similar construction  
274 results can be obtained without assuming a role for construction pheromone. We can hence ex-  
275 clude the influence of a cement pheromone, at least during the early choice of the deposition sites,  
276 in agreement with recent experiments by other authors (*Fouquet et al., 2014; Petersen et al., 2015;*  
277 *Green et al., 2017*). We should point to the fact, however, that in our experiments the building sub-  
278 strate was constantly moist throughout the entire duration of the experiments. It is possible that  
279 in some occurrences of nest building behavior, including in termites' natural environment, mois-  
280 ture may not constantly replenish the porous wall of the growing structure. We suggest that under  
281 these conditions the evaporation flux is maintained by the humidity that is naturally embedded in  
282 recently dropped pellets, which makes the construction process self-sustainable and is consistent  
283 with the hypothesis of a viscous boundary layer extending with termite activity (*Soar et al., 2019*).  
284 In practice, it would be very hard to distinguish between such a scenario and one which involves  
285 a putative cement pheromone added directly to manipulated pellets by termites. More generally,  
286 while we do not rule out a possible role of pheromones in termite building behavior (mediating for  
287 instance termite aggregation), we have shown that pheromones are not necessary to explain the  
288 early deposition patterns that we see in our experiments.

289 In this study we have focused on understanding how termites respond to well-controlled prede-  
290 fined stimuli. However, collective nest construction is a dynamic process and the deposition of new  
291 pellets by termites constantly changes the shape and the porosity of the evaporating substrate, po-  
292 tentially affecting nest growth through positive or negative feedback. Recent studies have shown  
293 that termites can control the size of the pellets used for nest construction, and indirectly also the  
294 porosity of nest walls (*Zachariah et al., 2017*). In turn, substrate porosity is known to play an impor-  
295 tant role for ventilation and drainage of the nest (*Singh et al., 2019*) and the moisture content of  
296 pellets can also affect the mechanical properties of the mound itself (*Zachariah et al., 2020*). In re-  
297 lation to our own experiments, however, our scaling analyses (SI S.IX) indicate that our conclusions  
298 are relatively robust to changes in substrate porosity and moisture content. For example, porosity  
299 only controls the time scale of water uptake from the reservoir by capillary rise, which must be  
300 small enough to keep the clay disk hydrated, and this assumption remains valid up to mm-size  
301 pores in the new construction. Similarly, for local curvature, the addition of new pellets to regions  
302 of high convexity is likely to make the surface less smooth than the initial topography, and such  
303 additional "roughness" can only increase the effect of focusing evaporation at those locations.

304 Previous work by Calovi and collaborators (*2019*) had pointed to an effect of surface curvature  
305 on termite construction behavior. While our two studies emphasize the same point, we should  
306 note that our results and the results reported in *Calovi et al. (2019)* are not entirely consistent, be-  
307 cause in our experiments, pellet depositions are attracted by convex features, while in *Calovi et al.*  
308 (*2019*) termite activity was concentrated at regions of maximum concavity. As this previous study  
309 did not distinguish digging from deposition activity, we believe that their measure is a correlation  
310 between concavity and digging activity, not building. The fact that concave regions should attract  
311 digging activity is predicted by our model (SI, section S.V) and was visible also in our experiments  
312 where concavity (Fig. 3D) attracted digging at the base of wall-like cues (SI, Fig. S2). Note that such  
313 behavior can be interpreted as termites digging along the humidity gradient, i.e. toward the most  
314 humid region. Accordingly, in many preliminary experiments we observed that, in the absence of  
315 loose pellets, spontaneous digging usually started right above the hydration holes of our setup (Fig.  
316 3B.)

317 In our study we have outlined a general mechanism capable of organizing termite building  
318 activity: termites would focus pellet depositions at regions of strong evaporation flux. In turn,

319 evaporation flux co-varies with surface curvature, which implies that the building rule is embedded  
320 in the shape itself of the nest internal structure.

321 One may wonder to what extent the simple building rule that we identify here generalizes to  
322 explain the nest-building behavior of larger termite colonies in the field, and whether the same  
323 building rules are shared across different termite species. The nests built by termites of different  
324 genera or species show a large diversity of forms (see e.g. *Grasse, 1984*), which indicates that the  
325 nest-building process should also be different. Arguably, the nest building behavior of termites,  
326 shaped by millions of years of evolution, must rely on more complex “building rules” than the  
327 simple ones highlighted here. Nonetheless, it is interesting to notice that the nests built by all  
328 species rely on a small number of architectural elements such as pillars and branching surfaces. We  
329 can imagine that, perhaps, simple variation of the basic building pattern described here, coupled  
330 with variation of the substrate evaporation itself (e.g. under the effect of air currents, the properties  
331 of the building material, and heat produced by the colony itself) would still be sufficient to explain  
332 a large part of termite nest diversity. Ocko and collaborators (*2019*) have already shown that a  
333 single mechanism can be responsible for determining the overall shape of nests made by various  
334 species: perhaps an equally simple general mechanism can account for the even larger variation  
335 of internal nest structure.

## 336 **Methods and Materials**

337 In our experiments, we monitor the building behaviour of small experimental groups of *Coptotermes*  
338 *formosanus* termites confronted with a thin layer of clay and pre-prepared clay features. We  
339 image experimental trials for their entire duration and we analyze termite activity with custom  
340 made digital image processing routines. In parallel we run two type of control experiments with-  
341 out termites to obtain a non-intrusive estimation of temperature, humidity and evaporation field  
342 in our experimental setup. These experiments are described at the end of this section.

### 343 **Experimental setup**

344 The experimental setup sketched Fig. 1 (left) can be described as follows. A fixed quantity (2.8 g)  
345 of red humid clay paste is flattened to form a disk ( $\varnothing$  5 cm) and placed in the center of a Petri dish  
346 ( $\varnothing$  8.5 cm). A system of 40 small holes ( $\varnothing$  0.8 mm) drilled in the bottom of the Petri dish keeps the  
347 clay paste hydrated sucking distilled water from a patch of wet cotton below the Petri dish. Two  
348 types of topographic cues molded in clay, can then be added at the center of the disk: 2 pillars 6  
349 mm high and 8 mm apart or 1 wall 6 mm high and 12 mm long. The pillars are obtained pressing  
350 clay in a small eppendorf tube. The walls are obtained by smoothing a wedge of clay generated by  
351 rolling out a piece of clay in the dihedral between the table and the edge of a plastic ruler. Finally,  
352 in a circular band (1 cm large) halfway between the clay disk center and its edge, we add 0.12 g of  
353 sparse pellets of gray clay. To ensure the good size distribution, pellets are obtained from previous  
354 experiments and sterilized at 100 °C for one hour to remove any possible chemical marker. Before  
355 the start of each experiment, a surface scan of the setup was taken using a NextEngine 3D Scanner  
356 ULTRA HD.

### 357 **Termite colonies**

358 Experimental groups were collected from a master captive colony of *Coptotermes formosanus* hosted  
359 at the LEEC laboratory (Villetaneuse, France) in a tropical room with constant temperature ( $26\pm 2$   
360 °C) and relative humidity ( $70\pm 10\%$ ), imitating their natural environment. Workers were attracted  
361 with humid towels and gently shoveled with a pencil on a plastic tray. Groups of 50 workers and  
362 5 soldiers were then formed using an insect forceps and added to an experimental setup. While  
363 the procedure might be potentially stressful to termites, mortality was negligible throughout all  
364 the experiments. We ran 16 experiments with pillar cues, 11 with a wall and 6 with no cues, as  
365 summarized in table S1 (SI).

## 366 Recordings

367 A led lamp constantly lightened the setup from above. Top view pictures of the experimental setups  
368 were taken at regular intervals of 20 seconds during at least 24 hours using a reflex camera Nikon  
369 D7500. By subtracting the initial images and applying a median filter, we get rid of termites and the  
370 background as detailed in SI section S.III. Then, the color contrast between the clay disk and the  
371 pellets allowed identifying where pellets were collected (dark spots) and deposited (bright spots)  
372 and building the heatmap of both activities as a function of time. A subset of the experiments was  
373 recorded continuously using a 12 Mp usb-Camera (MER2-1220-32U3C) at 7fps. Videos were then  
374 analyzed using the open-source tracking tool Trex (*Walter and Couzin, 2021*) and the occupancy  
375 frequency of termites computed in each part of the experimental setup.

## 376 Temperature and humidity measurements

377 Temperature and humidity were measured using a commercial temperature-humidity probe (DHT22)  
378 connected to a Raspberry Pi. To not interfere with termites behavior, our temperature and humid-  
379 ity measurements were performed in a control experiment which was prepared using the same  
380 protocol as the others but where no termites were added. The probe was kept at two different po-  
381 sitions that are i) at center of the experimental setup sitting on the clay disk and ii) at the periphery  
382 of the Petri dish, sitting on the bare plastic.

## 383 Growth model

384 Our growth model is the same described in *Facchini et al. (2020)* which consists in one single non-  
385 linear phase field equation:

$$\frac{\partial f}{\partial t} = -f(1-f)d\nabla \cdot \mathbf{n}f - \Delta \nabla \cdot \mathbf{n}. \quad (1)$$

386 where the scalar  $f$  takes values between 0 and 1 and identifies the presence of the nest wall ( $f <$   
387  $0.5$ ) or the empty space ( $f > 0.5$ ), and  $\mathbf{n} = \nabla f / |\nabla f|$  is the normal vector at the wall surface  $f = 0.5$ .  
388 One recognizes a growth term proportional to the surface curvature  $-\nabla \cdot \mathbf{n}/2$  which translates our  
389 main hypothesis on construction behaviour, and a curvature diffusion term  $\Delta \nabla \cdot \mathbf{n}$  which mimics the  
390 smoothing behaviour shown by termites (see *Facchini et al., 2020*, and citations inside) and the fact  
391 that there is a cutoff to the size of pellets added by termites. Finally, the non linear prefactor  $f(1-f)$   
392 restricts the growth process to the wall surface, which is also coherent with termites behaviour.  
393 Note that the simulations shown here are obtained approximating  $\nabla \cdot \mathbf{n} \approx \Delta f$  as in *Facchini et al.*  
394 *(2020)*. The parameter  $d$  selects the typical length scale of the expressed pattern and the cutoff  
395 scale below which features are smoothed out. Here, we tune the parameter  $d$  to select a typical  
396 length scale which matches that of our topographic cues, that is the thickness of our clay pillars  
397 and walls (3 mm).

398 Our simulation are initialized using 3D copies of the experimental setups at time zero that are  
399 obtained as it follows. First, we obtain a surface scan of the experimental setup in the form of a 3D  
400 mesh using a surface 3D scanner (see section S.III in the Supplementary Information). Then, we  
401 interpolate the mesh on a 3D regular grid and assign the initial value of the scalar field  $f$ , setting  
402  $f = 1$  for the points that are below the clay surface and  $f = 0$  for the points that are above the clay  
403 surface. Finally, a Gaussian filter is applied to unsharp the transition of  $f$  at the surface. Similarly  
404 to our previous publication, we also assume that the voxels where  $f > 0.85$  at  $t = 0$  cannot change  
405 in the following. This translates the fact that structures built by termites are not observed to be  
406 rearranged after they have dried and that in our experiments termites are prompted to collect  
407 pellets instead of digging.

## 408 Saline solution experiments

409 We performed control experiments with no termites and hydrating the clay disk with a saline so-  
410 lution instead of distilled water to map the distribution of evaporation flux. Saline solution was  
411 prepared adding 8 g of  $\text{NaCHO}_3$  to 100 ml of tap water.

## 412 Acknowledgments

413 We thank Paul Devienne at the LEEC laboratory for his help in taking care of termite colonies. We  
414 thank Baptiste Piqueret at LEEC laboratory for inspiring discussions. This work was supported by  
415 a Royal Society Newton International Fellowship NIF\R1\180238 and by a Leverhulme Research  
416 Project Grant RPG-2021-196.

## 417 References

- 418 **Bardunias P**, Su NY. Dead Reckoning in Tunnel Propagation of the Formosan Subterranean Termite (Isoptera:  
419 Rhinotermitidae). *Annals of the Entomological Society of America*. 2009; 102(1):158–165.
- 420 **Bardunias P**, Su NY. Opposing Headings of Excavating and Depositing Termites Facilitate Branch For-  
421 mation in the Formosan Subterranean Termite. *Animal Behaviour*. 2009 Sep; 78(3):755–759. doi:  
422 [10.1016/j.anbehav.2009.06.024](https://doi.org/10.1016/j.anbehav.2009.06.024).
- 423 **Bardunias PM**, Calovi DS, Carey N, Soar R, Turner JS, Nagpal R, Werfel J. The Extension of Internal Humidity Lev-  
424 els beyond the Soil Surface Facilitates Mound Expansion in Macrotermes. *Proceedings of the Royal Society*  
425 *B: Biological Sciences*. 2020 Jul; 287(1930):20200894. doi: [10.1098/rspb.2020.0894](https://doi.org/10.1098/rspb.2020.0894).
- 426 **Bardunias PM**, Su NY. Queue Size Determines the Width of Tunnels in the Formosan Subterranean Termite  
427 (Isoptera: Rhinotermitidae). *Journal of Insect Behavior*. 2010 May; 23(3):189–204. doi: [10.1007/s10905-010-](https://doi.org/10.1007/s10905-010-9206-z)  
428 [9206-z](https://doi.org/10.1007/s10905-010-9206-z).
- 429 **Bruinsma OH**. An Analysis of Building Behaviour of the Termite *Macrotermes Subhyalinus* (Rambur); 1979.
- 430 **Calovi DS**, Bardunias P, Carey N, Scott Turner J, Nagpal R, Werfel J. Surface Curvature Guides Early Construction  
431 Activity in Mound-Building Termites. *Philosophical Transactions of the Royal Society B: Biological Sciences*.  
432 2019 Jun; 374(1774):20180374. doi: [10.1098/rstb.2018.0374](https://doi.org/10.1098/rstb.2018.0374).
- 433 **Camazine S**, Deneubourg JL, Franks NR, Sneyd J, Theraulaz G, Bonabeau E. *Self-Organization in Biological*  
434 *Systems*, vol. 38. Princeton University Press; 2001. doi: [10.2307/j.ctvzxx9tx](https://doi.org/10.2307/j.ctvzxx9tx).
- 435 **Carey NE**, Bardunias P, Nagpal R, Werfel J. Validating a Termite-Inspired Construction Coordination  
436 Mechanism Using an Autonomous Robot. *Frontiers in Robotics and AI*. 2021 Apr; 8:645728. doi:  
437 [10.3389/frobt.2021.645728](https://doi.org/10.3389/frobt.2021.645728).
- 438 **Carey NE**, Calovi DS, Bardunias P, Turner JS, Nagpal R, Werfel J. Differential Construction Response to Hu-  
439 midity by Related Species of Mound-Building Termites. *The Journal of Experimental Biology*. 2019 Oct;  
440 222(20):jeb212274. doi: [10.1242/jeb.212274](https://doi.org/10.1242/jeb.212274).
- 441 **Deegan RD**, Bakajin O, Dupont TF, Huber G, Nagel SR, Witten TA. Capillary Flow as the Cause of Ring Stains  
442 from Dried Liquid Drops. *Nature*. 1997 Oct; 389(6653):827–829. doi: [10.1038/39827](https://doi.org/10.1038/39827).
- 443 **Facchini G**, Lazarescu A, Perna A, Douady S. A Growth Model Driven by Curvature Reproduces Geometric  
444 Features of Arboreal Termite Nests. *Journal of The Royal Society Interface*. 2020 Jul; 17(168):20200093. doi:  
445 [10.1098/rsif.2020.0093](https://doi.org/10.1098/rsif.2020.0093).
- 446 **Fouquet D**, Costa-Leonardo AM, Fournier R, Blanco S, Jost C. Coordination of Construction Behavior in the  
447 Termite *Procornitermes Araujoi*: Structure Is a Stronger Stimulus than Volatile Marking. *Insectes Sociaux*.  
448 2014 Aug; 61(3):253–264. doi: [10.1007/s00040-014-0350-x](https://doi.org/10.1007/s00040-014-0350-x).
- 449 **Grassé PP**. La reconstruction du nid et les coordinations interindividuelles chez *Bellicositermes natalensis* et  
450 *Cubitermes* sp. la théorie de la stigmergie: Essai d'interprétation du comportement des termites construc-  
451 teurs. *Insectes Sociaux*. 1959 Mar; 6(1):41–80. doi: [10.1007/BF02223791](https://doi.org/10.1007/BF02223791).
- 452 **Grasse PP**. *Termitologia Tome 2*. Fondation des sociétés, construction. Paris: Masson; 1984.
- 453 **Green B**, Bardunias P, Turner JS, Nagpal R, Werfel J. Excavation and Aggregation as Organizing Factors in de  
454 Novo Construction by Mound-Building Termites. *Proceedings of the Royal Society B: Biological Sciences*.  
455 2017 Jun; 284(1856):20162730. doi: [10.1098/rspb.2016.2730](https://doi.org/10.1098/rspb.2016.2730).
- 456 **Hansell M**. *Animal Architecture*. Oxford Animal Biology Series, Oxford, New York: Oxford University Press;  
457 2005.
- 458 **Heyde A**, Guo L, Jost C, Theraulaz G, Mahadevan L. Self-Organized Biotectonics of Termite Nests. *Proceedings*  
459 *of the National Academy of Sciences*. 2021 Feb; 118(5):e2006985118. doi: [10.1073/pnas.2006985118](https://doi.org/10.1073/pnas.2006985118).

- 460 **Hisatake K**, Tanaka S, Aizawa Y. Evaporation Rate of Water in a Vessel. *Journal of Applied Physics*. 1993 Jun;  
461 73(11):7395–7401. doi: [10.1063/1.354031](https://doi.org/10.1063/1.354031).
- 462 **Khuong A**, Gautrais J, Perna A, Sbai C, Combe M, Kuntz P, Jost C, Theraulaz G. Stigmergic Construction and  
463 Topochemical Information Shape Ant Nest Architecture. *Proceedings of the National Academy of Sciences*.  
464 2016 Feb; 113(5):1303–1308. doi: [10.1073/pnas.1509829113](https://doi.org/10.1073/pnas.1509829113).
- 465 **Khuong A**, Theraulaz G, Jost C, Perna A, Gautrais J. A Computational Model of Ant Nest Morphogenesis. In:  
466 *ECAL*; 2011. p. 411. doi: [10.13140/2.1.1334.1122](https://doi.org/10.13140/2.1.1334.1122).
- 467 **Langmuir I**. The Evaporation of Small Spheres. *Physical Review*. 1918 Nov; 12(5):368–370. doi: [10.1103/Phys-](https://doi.org/10.1103/PhysRev.12.368)  
468 [Rev.12.368](https://doi.org/10.1103/PhysRev.12.368).
- 469 **Ocko SA**, Heyde A, Mahadevan L. Morphogenesis of Termite Mounds. *Proceedings of the National Academy*  
470 *of Sciences*. 2019 Feb; 116(9):3379–3384. doi: [10.1073/pnas.1818759116](https://doi.org/10.1073/pnas.1818759116).
- 471 **Perna A**, Theraulaz G. When Social Behaviour Is Moulded in Clay: On Growth and Form of Social Insect Nests.  
472 *The Journal of Experimental Biology*. 2017 Jan; 220(Pt 1):83–91. doi: [10.1242/jeb.143347](https://doi.org/10.1242/jeb.143347).
- 473 **Petersen K**, Bardunias P, Napp N, Werfel J, Nagpal R, Turner S. Arrestant Property of Recently Manipulated Soil  
474 on *Macrotermes* *Michaelseni* as Determined through Visual Tracking and Automatic Labeling of Individual  
475 Termite Behaviors. *Behavioural Processes*. 2015 Jul; 116:8–11. doi: [10.1016/j.beproc.2015.04.004](https://doi.org/10.1016/j.beproc.2015.04.004).
- 476 **Singh K**, Muljadi BP, Raeini AQ, Jost C, Vandeginste V, Blunt MJ, Theraulaz G, Degond P. The Architectural Design  
477 of Smart Ventilation and Drainage Systems in Termite Nests. *Science Advances*. 2019 Mar; 5(3):eaat8520. doi:  
478 [10.1126/sciadv.aat8520](https://doi.org/10.1126/sciadv.aat8520).
- 479 **Soar R**, Amador G, Bardunias P, Turner JS. Moisture Gradients Form a Vapor Cycle within the Viscous Bound-  
480 ary Layer as an Organizing Principle to Worker Termites. *Insectes Sociaux*. 2019 May; 66(2):193–209. doi:  
481 [10.1007/s00040-018-0673-0](https://doi.org/10.1007/s00040-018-0673-0).
- 482 **Walter T**, Couzin ID. TRex, a Fast Multi-Animal Tracking System with Markerless Identification, and 2D Estima-  
483 tion of Posture and Visual Fields. *eLife*. 2021 Feb; 10:e64000. doi: [10.7554/eLife.64000](https://doi.org/10.7554/eLife.64000).
- 484 **Zachariah N**, Das A, Murthy TG, Borges RM. Building Mud Castles: A Perspective from Brick-Laying Termites.  
485 *Scientific Reports*. 2017 Dec; 7(1):4692. doi: [10.1038/s41598-017-04295-3](https://doi.org/10.1038/s41598-017-04295-3).
- 486 **Zachariah N**, Murthy TG, Borges RM. Moisture Alone Is Sufficient to Impart Strength but Not Weathering Resis-  
487 tance to Termite Mound Soil. *Royal Society Open Science*. 2020 Jul; 7(8):200485. doi: [10.1098/rsos.200485](https://doi.org/10.1098/rsos.200485).